previous evidence and the fact that in the present case it was by far the major fluorescent component of plant tRNA$^{Phe}$, we believe it to be a real constituent of tRNA$^{Phe}$. This is the first peroxy-Y base isolated from a higher plant source to have its structure determined.

**Acknowledgments.** We wish to thank Dr. George van Lear, Lederle Laboratories, for measurement of high-resolution mass spectra. This work has been supported by NIH Grant No. CA-11572, Hoffmann-La Roche Company (Columbia University), and Project 09.3.1 of the Polish Academy of Sciences.

### References and Notes

(1) (a) Columbia University; (b) Universytet im. Adama Mickiewicza.
(2) K. Nakanishi, N. Furutachi, M. Funamizu, D. Grunberger, and I. B. Weinstein, *J. Amer. Chem. Soc.*, **92**, 7617 (1970).
(3) M. Funamizu, A. Terahara, A. Feinberg, and K. Nakanishi, *J. Amer. Chem. Soc.*, **93**, 6706 (1971).
(4) H. Kasai, M. Goto, S. Takemura, T. Goto, and S. Matsaura, *Tetrahedron Lett.*, 2725 (1971).
(5) K. Nakanishi, S. H. Blobstein, M. Funamizu, N. Furutachi, G. van Lear, D. Grunberger, K. Lanks, and I. B. Weinstein, *Nature (London)*, **234**, 107 (1971).
(6) S. H. Blobstein, D. Grunberger, I. B. Weinstein, and K. Nakanishi, *Biochemistry*, **12**, 188 (1973).
(7) U. L. RajBhandary, S. H. Chang, A. Stuart, R. C. Faulkner, R. M. Hoskinson, and H. G. Khorana, *Proc. Nat. Acad. Sci. U.S.*, **57**, 751 (1967).
(8) R. Thiebe and H. G. Zachau, *Eur. J. Biochem.*, **5**, 546 (1968).
(9) F. L. Suddath, G. J. Quigley, A. McPherson, D. Sneden, J. J. Kim, S. H. Kim, and A. Rich, *Nature (London)*, **248**, 20 (1974).
(10) H. J. Li, K. Nakanishi, D. Grunberger, and J. B. Weinstein, *Biochem. Biophys. Res. Commun.*, **55**, 818 (1973).
(11) D. Yoshikami, G. Katz, E. B. Keller, and B. S. Dudock, *Biochim. Biophys. Acta*, **166**, 714 (1968).
(12) C. W. Hancher, C. F. Phares, G. D. Norelli, and A. D. Kelmers, *Biotechnol. Bioeng.*, **11**, 1055 (1969).
(13) D. W. Thomas and K. Biemann, *J. Amer. Chem. Soc.*, **87**, 5447 (1965).
(14) This aspect will be discussed elsewhere; manuscript in preparation.
(15) J. E. van Lear and L. L. Smith, *J. Org. Chem.*, **36**, 1007 (1971).
(16) M. H. Abraham, A. G. Davies, D. R. Llewellyn, and E. M. Thain, *Anal. Chim. Acta*, **17**, 499 (1957).

# Contribution of Side Chain Chromophores to the Optical Activity of Proteins. Model Compound Studies. II. p-Hydroxyphenylglycine and p-Hydroxyphenylglycinamide

**Julian W. Snow and Thomas M. Hooker, Jr.***

*Contribution from the Department of Chemistry, University of California, Santa Barbara, California. 93106. Received April 26, 1974*

**Abstract:** The optical properties and conformational stability of p-hydroxyphenylglycine and p-hydroxyphenylglycinamide have been investigated. The rotatory strengths associated with the electronic transitions of the chromophores of these molecules have been computed as a function of molecular conformation. The theoretical rotatory strengths have been used in conjunction with semiempirical conformational energy calculations and experimental optical rotatory dispersion and circular dichroism data to determine the conformation of these molecules in solution. The results of this investigation indicate that both molecules assume conformations for which the dihedral angle $\psi$ assumes values near $-5°$ and the dihedral angle $\chi$ assumes values near 75°.

An understanding of the origin of the Cotton effects of amino acids and amino acid derivatives with side chains having chromophores with electronic transitions between 200 and 300 nm is of interest because of their possible function as a conformational probe in proteins. Model compound studies involving aromatic amino acids[1] and cyclic dipeptides[2] have been carried out previously. Experimental and theoretical spectroscopic investigations were performed on these molecules, as well as theoretical calculations of conformational potential energies, in an attempt to correlate their optical properties with conformation.

This paper reports the results of similar investigations on p-hydroxy-L-phenylglycine (α-amino-p-hydroxyphenylacetic acid) and p-hydroxy-L-phenylglycinamide. This amino acid was selected for study because although it is closely related to L-tyrosine, which was studied previously,[1] it is much simpler from a structural point of view. Since the aromatic ring is directly bonded to the α-carbon atom, significant stereochemical interactions should occur between the γ-hydrogen atoms of the aromatic ring and the bulky carbonyl and amino functions. Thus, the conformational freedom of these molecules should be severely restricted. Furthermore, the conformation of p-hydroxyphenylglycine and p-hydroxyphenylglycinamide can be described with one less dihedral angle than is required for the more common aromatic amino acids, so theoretical calculations are commensurately simpler. Thus, the results of these calculations should provide a good test of the theoretical techniques which are used.

## Experimental Section

**Procedure.** The enantiomeric isomers of p-hydroxyphenylglycine were donated by J. H. C. Nayler. p-Hydroxy-D- and -L-phenylglycinamide were prepared from the amino acids by standard techniques. The amides showed only one spot when subjected to thin-layer chromatography on silica gel in acetic acid–butanol–water. Elemental analysis for carbon, hydrogen, and nitrogen showed no deviations from theoretical values greater than 0.11%. In addition, the low resolution mass spectra of both optical isomers of the amide were consistent with the products being authentic.

All samples were dried over silica gel prior to preparation of solutions. Solutions were prepared in volumetric flasks with doubly distilled water. Samples were weighed to the nearest hundredth milligram.

Absorption spectra were measured on a Cary 118C (far uv model) recording spectrophotometer. Optical rotatory dispersion (ORD) and circular dichroism (CD) spectra were measured on a Cary 60 recording spectropolarimeter equipped with a prototype Model 6003 circular dichroism accessory. Spectra were recorded at various scan rates with appropriate corresponding pen periods or time constants. The instrument slits were programmed to yield a constant spectral resolution of 15 Å. Fused silica cells with path lengths between 0.1 and 5.0 cm were used.

Optical rotation and circular dichroism data are reported as

molar rotation, $M_\alpha$, and molar ellipticity, $M_\theta$, which are defined by

$$\alpha = M_\alpha Cl/100$$

and

$$\theta = M_\theta Cl/100$$

where $\alpha$ is the observed optical rotation in degrees, $\theta$ is the observed ellipticity in degrees, $l$ is the cell path length in centimeters, and $C$ is the concentration of solute in moles per liter.

Computations and theoretical calculations were carried out on the IBM 360/75 computer of the University of California, Santa Barbara, computer center.

## Methods

The conformation of p-hydroxy-L-phenylglycine is defined following the conventions proposed by Edsall, *et al.*[3] Figure 1 shows an illustration of p-hydroxy-L-phenylglycine in the $\psi = 0°$, $\chi = 80°$ conformation. The zero dihedral angle conformation ($\psi = \chi = 0$) was the starting conformation for these calculations. In this conformation the N–$C^\alpha$ and $C'$–$O'^2$ bonds are eclipsed for $\psi$ equal zero, as are the N–$C^\alpha$ and $C^\beta$–$C^\gamma$ bonds for $\chi$ equal zero. The amino group is oriented such that $H^{N_1}$ is in the plane of the aromatic ring and trans to $C^\beta$, *i.e.*, the N–H bonds are staggered with respect to the bonds on $C^\alpha$. It was assumed that rotation about $\varphi$ does not significantly affect the conformation of the remainder of the molecule; therefore $\varphi$ was not varied in these calculations.

Atomic coordinates for both p-hydroxy-L-phenylglycine and p-hydroxy-L-phenylglycinamide were based on the X-ray diffraction data of Srinivasan[4] for L-tyrosine. Obvious distortions, *e.g.*, unequal bond distances within the phenyl ring, were eliminated using idealized bond distances and bond angles as proposed by Pauling.[5] Standard bond angles and bond distances were also assumed for the calculation of atomic coordinates for the amide group. The atomic coordinates which were utilized in this investigation are listed in Table I.

**Table I.** Coordinates and Static Charges for p-Hydroxy-L-phenylglycine and p-Hydroxy-L-phenylglycinamide ($\varphi = \psi = \chi = 0°$)

| Atom | Atomic coordinates, Å | | | Static charge[a] | |
| | $x$ | $y$ | $z$ | Amino acid | Amide |
|---|---|---|---|---|---|
| $C^\epsilon$ | 0.0 | 0.0 | 4.313 | 0.666 | 0.666 |
| $C^{\delta_1}$ | 0.0 | 1.210 | 3.615 | -0.455 | -0.455 |
| $C^{\delta_2}$ | 0.0 | -1.210 | 3.615 | -0.455 | -0.455 |
| $C^{\gamma_1}$ | 0.0 | 1.210 | 2.218 | -0.229 | -0.231 |
| $C^{\gamma_2}$ | 0.0 | -1.210 | 2.218 | -0.229 | -0.231 |
| $C^\beta$ | 0.0 | 0.0 | 1.519 | -0.110 | -0.123 |
| $C^\alpha$ | 0.0 | 0.0 | 0.0 | 0.302 | 0.270 |
| $C'$ | -1.261 | -0.727 | -0.515 | 1.171 | 1.596 |
| $H^\zeta$ | 0.0 | 0.703 | 6.176 | 1.457 | 1.457 |
| $H^{\delta_1}$ | 0.0 | 2.148 | 4.157 | 0.258 | 0.258 |
| $H^{\delta_2}$ | 0.0 | -2.148 | 4.157 | 0.258 | 0.258 |
| $H^{\gamma_1}$ | 0.0 | 2.148 | 1.676 | 0.254 | 0.254 |
| $H^{\gamma_2}$ | 0.0 | -2.148 | 1.676 | 0.254 | 0.254 |
| $H^\alpha$ | 0.898 | -0.518 | -0.367 | 0.252 | 0.241 |
| $H^{N_1}$ | 0.0 | 1.394 | -1.539 | 1.189 | 0.945 |
| $H^{N_2}$ | 0.849 | 1.877 | -0.158 | 1.189 | 0.945 |
| $H^{N_3}$ | -0.849 | 1.877 | -0.158 | 1.189 | 0.945 |
| N | 0.0 | 1.392 | -0.498 | 0.632 | 1.549 |
| $O^\zeta$ | 0.0 | 0.0 | 5.688 | -1.663 | -1.663 |
| $O'^1$ | -1.418 | -1.936 | -0.180 | -2.965 | |
| $O'^2$ | -2.060 | -0.070 | -1.242 | -2.965 | |
| N' | -1.424 | -1.989 | -0.165 | | -1.802 |
| O' | -2.042 | -0.079 | -1.228 | | -2.011 |
| $H^{N_1'}$ | -0.770 | -2.478 | 0.411 | | 1.068 |
| $H^{N_2'}$ | -0.210 | -2.532 | -0.454 | | 1.068 |

[a] The units of charge are $10^{-10}$ esu; *i.e.*, the charge of the electron is $-4.8$ in these units. The charges listed for the amide are for the protonated species.
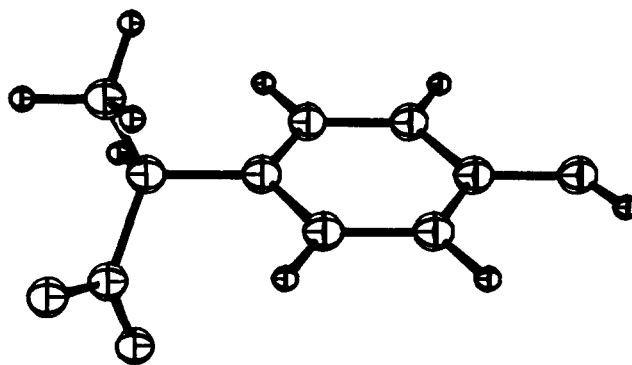


**Figure 1.** Illustration of p-hydroxy-L-phenylglycine in the $\psi = 0°$, $\chi = 80°$ conformation.

Semiempirical conformational energy calculations were carried out by standard methods similar to the procedures developed by Flory,[6] Scheraga,[7] and Ramachandran.[8] The calculated energies include contributions from nonbonded and electrostatic interactions. These interactions are represented by the Lennard-Jones "6-12" function and a Coulomb's law function, respectively. These potentials are given by

$$V_{i,j} = \frac{-a_{ij}}{r^6_{ij}} + \frac{b_{ij}}{r_{ij}^{12}} \tag{1}$$

$$V_{el} = \sum_{i,j} \frac{K(q_i q_j)}{\epsilon r_{ij}} \tag{2}$$

where $r_{ij}$ is the interatomic distance in Å, $a_{ij}$ and $b_{ij}$ are adjustable parameters, $q_i$ is the static charge on atom $i$, $\epsilon$ is the apparent dielectric constant, and $K$ is a conversion factor that is dependent upon the units of $q$ and $r$.

The method of Ooi, *et al.*,[9] was utilized to investigate the effect of barriers to internal rotation upon the conformational freedom of these molecules. Because of the relatively low barrier heights for the bonds under consideration, torsional interactions were found to be negligible in comparison to nonbonded and electrostatic interactions. Since electrostatic and nonbonded interactions are clearly dominant in determining the conformational preferences for these molecules, the contribution of torsional barriers to the total conformational energy was eliminated from the results reported herein.

The parameters used in the Lennard-Jones function were taken from the work of Ooi, *et al.*[9] The static charges used in the electrostatic energy calculations are presented in Table I. These charges include contributions from both $\sigma$ and $\pi$ orbitals. The total static charge for each atom is the sum of $\sigma$ and $\pi$ contributions. The methods of Del Re[10] and Berthod and Pullman[11] were used for the calculation of these charges. The static charges of the amide group were taken from the work of Poland and Scheraga.[12]

Since p-hydroxy-L-phenylglycine is zwitterionic at neutral pH, the charges listed in Table I include a charge of $-0.5$ e added to both carboxylate oxygen atoms and $+1$ e added to the nitrogen atom. A charge of $+1$ e has also been added to the amino nitrogen of p-hydroxy-L-phenylglycinamide.

A value of unity was chosen for the dielectric constant in eq 2. This value is unrealistically low, except for contacts approaching the van der Waals radius. However, alternative values for the dielectric constant represent a change only in the scaling factor of the electrostatic potential energy and will not alter the shape of the electrostatic energy contour. Nevertheless, the effect of higher dielectric con-
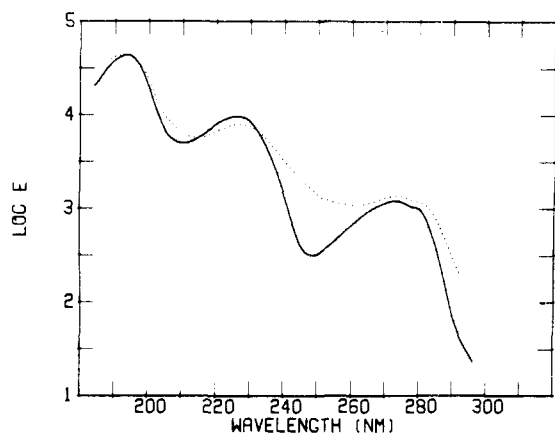
Figure 2. Ultraviolet absorption spectra of p- hydroxy-L-phenylglycine (——) and p- hydroxy-L-phenylglycinamide (· · ·) in aqueous solution.

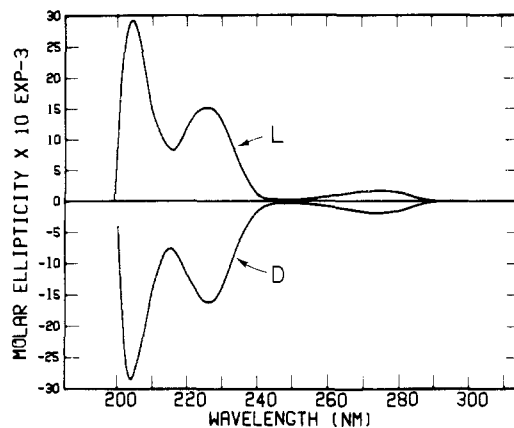

Figure 3. Circular dichroism spectra of p- hydroxyphenylglycine in neutral aqueous solution. The upper curve is the L isomer and the lower curve is the D isomer.

stants was investigated by carrying out calculations for p- hydroxy-L-phenylglycine with an effective dielectric constant of 3.

There are at least three interaction mechanisms that are known to be of importance in explaining the optical activity of molecules which contain intrinsically symmetric chromophores. One of these, the coupled oscillator mechanism of Kirkwood,[13] Kuhn,[14] and Moffitt,[15] involves the coupling of the electric transition dipole moments of two electronic transitions. The $\mu$-m mechanism involves the coupling of a magnetically allowed transition of one chromophore with an electrically allowed transition of another chromophore.[16-19] The one-electron mechanism of Condon, Altar, and Eyring[20] involves the mixing of a magnetically allowed transition with an electrically allowed transition on the same chromophore, under the perturbation due to the asymmetric static field arising from the remainder of the molecule.

The optical calculations that were carried out in this investigation are based on a matrix theory of optical activity which incorporates these three interaction mechanisms. The theory and application of this matrix formalism have been described elsewhere for simple amides[16] and for tyrosine.[1]

The directions and magnitudes of the electronic transition moments of the phenolic and carboxylate chromophores of p- hydroxyphenylglycine were assumed to be identical with those of tyrosine which have been described in detail elsewhere.[1] In brief, the four lowest energy absorption bands of the phenolic chromophore have been included in these calculations. In Platt's[21] notation these are the $^1L_b$ band at 272 nm, which lies in the plane of the aromatic ring, polarized perpendicular to the $C_2$ rotation axis of the ring, the $^1L_a$ band at 226 nm, which lies in the plane of the ring, polarized parallel to the $C_2$ axis, and the near degenerate $^1B_b$ and $^1B_a$ bands which appear in phenol as one band at 190 nm with a shoulder slightly to the blue. These assignments are based on the spectral assignments of benzene first proposed by Goeppert-Mayer and Sklar.[22] The magnitudes of these aromatic transition dipole moments and their associated charge monopoles were determined by means of a semiempirical Pariser-Parr-Pople SCF-MO calculation with limited configuration interaction.[1]

Only the lowest energy $\pi \rightarrow \pi^*$ transition of the carboxylate group has been included in these calculations. The energy of this transition was taken from the data of Barnes and Simpson[23] to be 173 nm, which is in reasonable agreement with the more recent results of Snyder, et al.[24] This transition should be polarized along a line between the oxygen atoms in the $O'^1$-$C'$-$O'^2$ plane. The magnitude of the transition moment was taken to be 2.6 D.[1]

The magnetically allowed n-$\pi^*$ transition of the carboxylate group, which probably occurs slightly above 200 nm,[24] should have only a slight effect on the optical activity of the lower energy aromatic bands because the only appropriate mechanism for the interaction of magnetically allowed transitions with electrically allowed transitions is the $\mu$-m mechanism. Since this mechanism involves a dipole-quadrupole interaction, it would not be expected to contribute significantly to the optical activity of transitions as widely separated in energy as these. Thus, since the n-$\pi^*$ transition of the carboxylate group is not well characterized, it has not been included in these calculations.

Both the n-$\pi^*$ and $\pi$-$\pi^*$ transitions of the amide chromophore were included in the theoretical calculations. The energies of these transitions were chosen to be 212 and 183 nm, respectively, after Nielsen and Schellman.[25] The direction of the amide $\pi$-$\pi^*$ transition moment was obtained from the polarized absorption studies of Peterson and Simpson.[26] The value of 2.8 D was taken as the magnitude of this transition moment.[25,27]

The direction of the magnetic moment that is associated with the n $\rightarrow$ $\pi^*$ transition of the amide chromophore is along the $C'$-O axis. The magnitude of this transition moment is taken to be 1.167 B.[27] The charge monopoles associated with the amide transitions were taken from the work of Bayley, et al.[16]

## Results

The uv absorption spectrum of p- hydroxy-L-phenylglycine in aqueous solution is shown in Figure 2. The absorption bands near 273 and 226 nm are assigned to the $^1L_b$ and $^1L_a$ transitions, respectively. The $^1B$ bands of the aromatic chromophore are probably responsible for the absorption maximum that occurs near 194 nm.

Figure 2 also shows the uv absorption spectrum for p- hydroxy-L-phenylglycinamide. The $^1L_b$ and $^1L_a$ bands are shifted to the red about a nanometer relative to their wavelengths in the free amino acid. Again, the $^1B$ bands are probably responsible for the absorption maximum near 194 nm. The weak n-$\pi^*$ transition of the amide group is hidden by these intense aromatic bands.

The $\pi$-$\pi^*$ transitions of the amide and carboxylate groups should occur below 190 nm; hence these bands should make only a background contribution in the low wavelength region of the absorption spectra shown in Figure 2.

The CD spectra of both the L and D isomers of p- hydroxyphenylglycine in aqueous solution are shown in Figure 3. The ORD spectrum of the L isomer is presented in Figure 4.
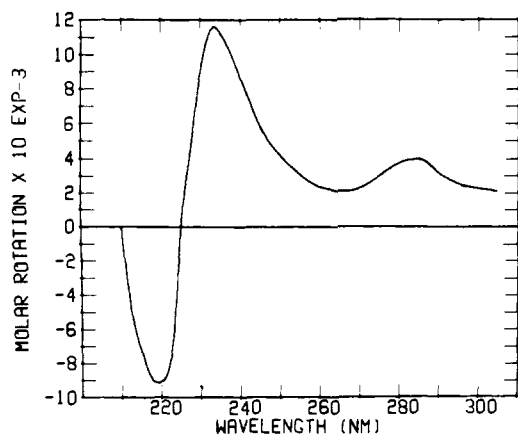
**Figure 4.** Optical rotatory dispersion spectrum of p- hydroxy-L-phenyl-glycine in neutral aqueous solution.
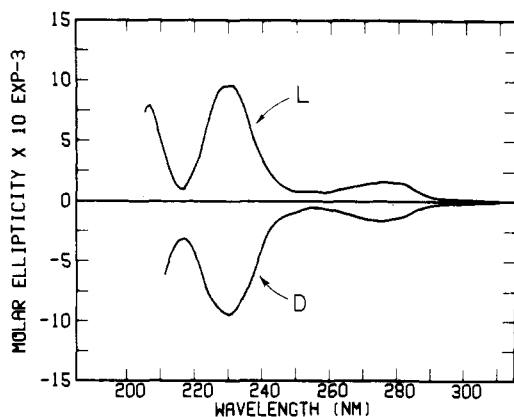


**Figure 5.** Circular dichroism spectra of p- hydroxyphenylglycinamide in aqueous solution, pH 5. The upper curve is the L isomer and the lower curve is the D isomer.



**Figure 6.** Optical rotary dispersion spectrum of p- hydroxy-L-phenyl-glycinamide in aqueous solution, pH 5.



**Figure 7.** Nonbonded energy contour map for p- hydroxy-L-phenylgly-cine. Highest contour line represents an arbitrary zero of energy. Contours are spaced at 1-kcal intervals.

Both the CD and ORD spectra of the L isomer indicate the presence of two positive Cotton effects centered at 273 and 226 nm. These Cotton effects undoubtedly arise from the $^1L_b$ and $^1L_a$ bands, respectively. There is a third Cotton effect (positive in the L isomer) with an apparent extremum near 204 nm. It is impossible to make a definite assignment for this Cotton effect since it might arise from one of the $^1B$ transitions of the phenolic chromophore or from the n–$\pi^*$ transition of the carboxylate group. The sharpness of the CD band on the low wavelength side provides evidence of a Cotton effect of opposite sign to the blue. This Cotton effect might arise from one of the higher energy aromatic transitions or from the $\pi$–$\pi^*$ transition of the carboxylate group.

The CD spectra of the L and D isomers of p- hydroxy-phenylglycinamide appear in Figure 5. The ORD spectrum of the L isomer is shown in Figure 6. The pH of these solutions was lowered to 5 to ensure protonation of the amino nitrogen. Since the apparent $pK_a$ of the amide was determined to be 7.1 by titration, there should be a large excess of the protonated form at this pH. The CD spectrum of the amide was also determined at pH 9.15. Positive Cotton effects were observed near 275, 226, and 208 nm. These Cotton effects were slightly weaker than the analogous bands at pH 5, but qualitatively the spectrum was similar to the lower pH spectrum. The Cotton effects at 275 and 226 nm are assigned to the $^1L_b$ and $^1L_a$ bands, respectively. As in the case of the amino acid, there is a third Cotton effect, which is partially resolved, to the blue of the $^1L_a$ band.

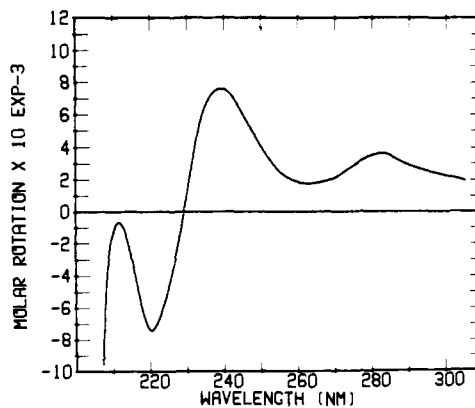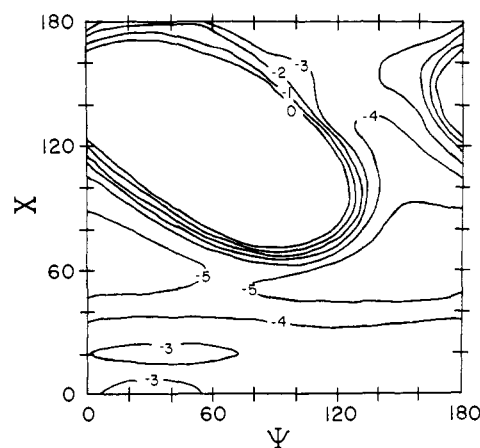The ORD spectrum of the L isomer of the amide (Figure 6) also indicates the presence of a positive band to the blue

of the $^1L_a$ band. In addition, the ORD spectrum definitely shows the presence of an intense negative band below 210 nm. More recent CD data confirm the presence of an intense negative band below 200 nm. As was the case with the amino acid, it is not possible to make definitive assignments for these two lower wavelength bands.

The results of the conformational energy calculations for the p- hydroxy-L-phenylglycine molecule are presented as conformational energy contour maps. The abscissa and ordinate of each map are the dihedral angles $\psi$ and $\chi$. As a result of the $C_2$ symmetry axes of the phenyl and carboxylate groups, these angles were varied only over the range from 0 to 180°. The energy difference between adjacent contour lines corresponds to 1 kcal/mol. The energy scale for each map has been arbitrarily adjusted so that the energy of the highest contour line corresponds to 0 kcal/mol.

The nonbonded and electrostatic energy contour maps for p- hydroxy-L-phenylglycine are presented in Figures 7 and 8, respectively. The large nonbonded energy barrier for values of $\chi$ greater than 80–100° is due to repulsive interactions of the carboxylate group with the phenolic ring. A smaller electrostatic barrier centered near $\psi$ = 90°, $\chi$ = 0° (Figure 8) hinders rotation about $\psi$ for values of $\chi$ less than 60°. This barrier is of indeterminable height as it depends upon the effective dielectric constant, the value of which is not accurately known.

A potential energy contour map for the sum of nonbonded and electrostatic interactions of p- hydroxy-L-phenylglycine is presented in Figure 9. This map indicates that the most stable conformers of this molecule should have $\psi$
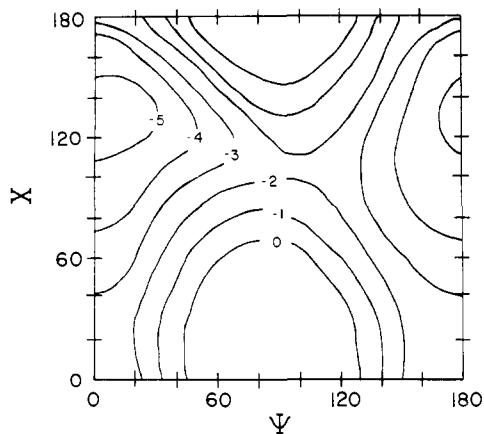
**Figure 8.** Electrostatic potential energy contour map for *p*-hydroxy-L-phenylglycine. Energies are relative to an arbitrary zero. Contours are spaced at 1-kcal intervals.
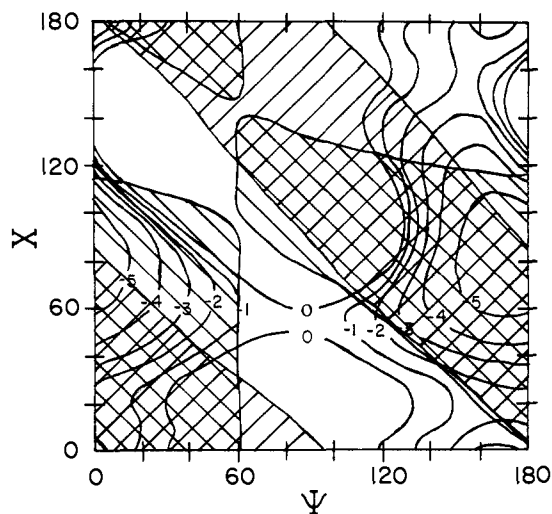


**Figure 9.** Rotatory strength–total conformational energy map for *p*-hydroxy-L-phenylglycine. Energies are relative to an arbitrary zero. Lines enclosing shaded areas are nodal lines for rotatory strength. Crosshatched regions indicate positive rotatory strength for both the $^1L_b$ and $^1L_a$ transitions; shading with positive slope indicates positive rotatory strength for the $^1L_b$, negative for the $^1L_a$; shading with negative slope indicates negative $^1L_b$, positive $^1L_a$; in unshaded areas both Cotton effects are predicted to be negative.

values between 150 and 195° (−30 and 15°) and $\chi$ values between 60 and 100°.

Superimposed on the total energy contour map are nodal lines of rotatory strength calculated for the $^1L_b$ and $^1L_a$ absorption bands of the phenolic chromophore. The areas of conformation space for which positive rotatory strength is predicted are shaded. Crosshatched conformations indicate positive Cotton effects for both the $^1L_b$ and $^1L_a$ bands; shading with positive slope represents positive rotatory strength for the $^1L_b$ band, negative for the $^1L_a$ band; shading with negative slope represents negative $^1L_b$, positive $^1L_a$; in blank areas both Cotton effects are predicted to be negative. There is one contiguous region of conformation space in which the predicted rotatory strength for both of the lower energy aromatic absorption bands is positive, as was experimentally observed to be the case. This region appears on the map as the three crosshatched areas that occur near $\psi = 30°, \chi = 30°, \psi = 40°, \chi = 170°$, and $\psi = 140°, \chi = 60°$.

Figures 10 and 11 illustrate the nonbonded and electrostatic energy contour maps for *p*-hydroxy-L-phenylglycinamide. Note that $\psi$ is varied from 0 to 360° for this molecule
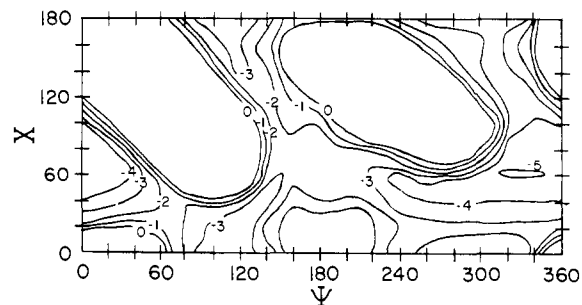


**Figure 10.** Nonbonded energy contour map for *p*-hydroxy-L-phenylglycinamide. The highest contour line represents an arbitrary zero of energy. Contours are spaced at 1-kcal intervals.

because the amide group does not possess a twofold axis of symmetry. The large nonbonded barriers that are centered near $\psi = 60°, \chi = 120°$ and $\psi = 240°, \chi = 120°$ are due to repulsive interactions involving atoms of the phenolic ring and atoms of the amino and carbonyl functions of the amide group, respectively. Figure 11 indicates that there is a broad area of electrostatic repulsion for all values of $\psi$ between approximately 60 and 300°. This is a result of repulsive electrostatic interactions involving the hydrogen atoms of the amide and amino functions. The barrier is again of indeterminable height, although it is obviously higher than the electrostatic barrier to rotation about $\psi$ in *p*-hydroxy-L-phenylglycine.

The total conformational energy–rotatory strength map for *p*-hydroxy-L-phenylglycinamide is shown in Figure 12. The lowest energy contour line on this map indicates that the most stable conformations of this molecule should have $\psi$ values between 345 and 375° and $\chi$ values between 55 and 95°.

As in the case of the amino acid, nodal lines for the rotatory strength of the aromatic $^1L_b$ and $^1L_a$ bands have been superimposed on the conformational energy contour map. Again, the crosshatched areas denote conformations which are predicted to yield positive rotatory strengths for both bands. Thus, there are five areas in Figure 12 which correspond to conformations that are predicted to yield the experimentally observed positive rotatory strengths for the two lowest energy absorption bands of the phenolic chromophore of *p*-hydroxy-L-phenylglycinamide.

**Discussion**

Semiempirical conformational energy calculations such as those carried out in this work are at best of uncertain accuracy. There are several possible sources of error which are inherent in such calculations. One of these, *i.e.*, the choice of a value for the effective dielectric constant, has already been mentioned. However, in the present instance this is probably not a serious source of error. The total conformational energy contour map which was obtained when an effective dielectric constant of 3 was utilized for the electrostatic energy calculations was identical with the one obtained with a dielectric constant of unity. This is to be expected, since consideration of Figures 7, 8, and 9 clearly indicates that the nonbonded interactions are dominant in the case of *p*-hydroxy-L-phenylglycine; *i.e.*, the position of the energy minimum in Figure 9 is approximately the same as the position of the nonbonded energy minimum in Figure 7. The problem is even less serious in the case of *p*-hydroxy-L-phenylglycinamide, since the electrostatic energy minimum falls at practically the same location in the conformation space as the nonbonded energy minimum. Thus, the value of the effective dielectric constant has a minimal ef-
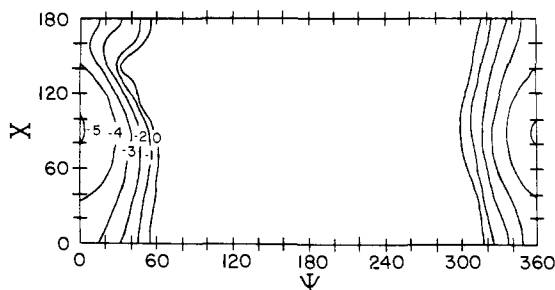
Figure 11. Electrostatic potential energy contour map for $p$-hydroxy-L-phenylglycinamide. Energies are relative to an arbitrary zero. Contours are spaced at 1-kcal intervals.



Figure 12. Rotatory strength–total conformational energy map for $p$-hydroxy-L-phenylglycinamide. Energies are relative to an arbitrary zero. Lines enclosing shaded areas are nodal lines for rotatory strength. Crosshatched regions indicate positive rotatory strength for both the $^1L_b$ and $^1L_a$ transitions; shading with positive slope indicates positive rotatory strength for the $^1L_b$, negative for the $^1L_a$; shading with negative slope indicates negative $^1L_b$, positive $^1L_a$; in unshaded areas both Cotton effects are predicted to be negative.

fect upon the predictions of the conformational energy calculations for these particular molecules.

However, there are other potential sources of error which might have significant effects upon the results. For example, solvent effects have been completely ignored, the validity of the semiempirical parameters which were used is uncertain, and there can be no assurance that the chosen energy functions actually reproduce the interatomic forces they are supposed to represent.

In spite of these limitations to the accuracy of these calculations, they can be very useful as guides for the determination of the approximate relative stability of various conformers and as a measure of the approximate significance of specific classes of interatomic interactions. When used in such a nonquantitative way in conjunction with experimental spectroscopic probes of molecular conformation, semiempirical conformational energy calculations can be very useful for the conformational analysis of simple molecules in solution.

The nonbonded, electrostatic, and total energy maps for $p$-hydroxy-L-phenylglycine are quite similar to those for $p$-hydroxy-L-phenylglycinamide. Examination of these energy contour maps indicates that for small values of $\chi$ electrostatic interactions appear to be responsible for restricting rotational freedom about the dihedral angle $\psi$ in both the free amino acid and the amide. Repulsive electrostatic interactions which occur between the hydrogen atoms of the amide and amino groups are responsible for the predicted instability of the $\psi = 180°$ conformers in $p$-hydroxy-L-phenylglycinamide. However, as is evident from Figure 10, the nonbonded energy for the amide is also slightly higher for $\psi = 180°$ than for $\psi = 0°$, primarily as a result of contacts between these same atoms.

Nonbonded contacts appear to be responsible for restricting the freedom of rotation about the dihedral angle $\chi$. As might be expected, strong repulsive interactions occur between the $\gamma$-hydrogen atoms of the aromatic ring and the bulky carbonyl and amino substituents on the $\alpha$-carbon atom in both the amino acid and the amide.

As was pointed out earlier, the electrostatic interactions and nonbonded interactions reinforce one another insofar as $p$-hydroxy-L-phenylglycinamide is concerned, that is they appear to give rise to energy minima in roughly the same region of the conformation space. This is not the case for the free amino acid. In the case of $p$-hydroxy-L-phenylglycine, the minimum in electrostatic energy occurs at $\chi$ values near 130°, whereas the minimum in nonbonded energy is predicted to fall near $\chi = 70°$. However, the electrostatic energy well is quite shallow along the $\chi$ axis, so the nonbonded interactions are dominant and play the major role in determining the position of the energy minimum on the total energy contour map. Thus, it seems reasonable to infer that the total energy contour maps for both the free amino
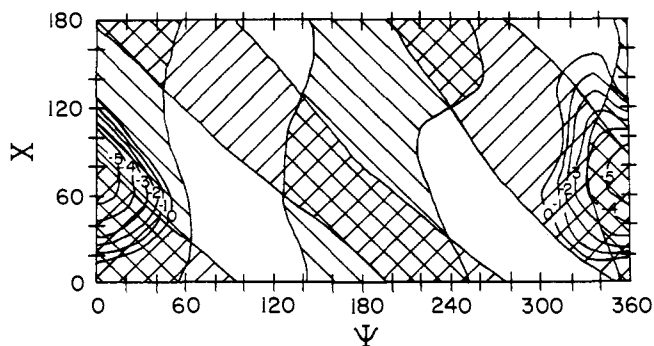
acid and the amide probably give a fairly accurate location of the conformational energy minima for the respective molecules. The total conformational energy maps for $p$-hydroxy-L-phenylglycine (Figure 9) and $p$-hydroxy-L-phenylglycinamide (Figure 12) predict that the most stable conformers for both molecules should occur in essentially the same region of the corresponding conformation spaces, i.e., near $\psi = -5°$ (175°), $\chi = 80°$ for the free amino acid, and near $\psi = -5°$ (355°), $\chi = 70°$ for the amide.

It is significant that the energy minima on the contour maps for both $p$-hydroxy-L-phenylglycine and $p$-hydroxy-L-phenylglycinamide fall generally within an area of conformation space for which the optical calculations predict the experimentally observed rotatory strengths for both the $^1L_b$ and $^1L_a$ bands of the phenolic chromophore, i.e., the crosshatched areas of Figures 9 and 12. Even if the conformational energy calculations are in error by considerably more than 5 kcal, the results of the optical calculations still indicate that the conformational freedom of both $p$-hydroxy-L-phenylglycine and $p$-hydroxy-L-phenylglycinamide is restricted and is confined to a relatively small area of conformation space in the vicinity of $\psi = -5°$, $\chi = 75°$. However, it should not be inferred that other conformations are absolutely inaccessible at ordinary temperatures. Although the data of Figures 9 and 12 indicate that the energy contours are relatively steep, it must be recognized that molecular geometry was not permitted to relax in these calculations, i.e., covalent bonds were treated as rigid rods. Thus, the calculated repulsive energies are probably overestimated for many of the sterically unfavorable conformations. Nevertheless, it certainly appears that conformations with $\psi$ near $-5°$ and $\chi$ near 75° must be the most heavily populated ones.

The uncertainties associated with the semiempirical conformational energy calculations should not detract from the beautiful agreement between experiment and theory. For example, the observed rotatory strengths for the $^1L_b$ and $^1L_a$ bands of $p$-hydroxy-L-phenylglycine were determined by curve fitting to be 0.01 and 0.1 DB, respectively. In the case of the amide, the corresponding experimental values were 0.01 and 0.05, respectively. The theoretical rotatory strengths for the amino acid with $\psi = -5°$, $\chi = 75°$ are 0.005 and 0.06 for the $^1L_b$ and $^1L_a$ bands, respectively. For the amide the corresponding values are 0.006 and 0.04. Thus, the agreement between theory and experiment is really quite good. In fact, the agreement could readily be made quantitative if the conformational angles were regarded as adjustable parameters.

**Table II.** Comparison of Theoretical and
Experimental Rotatory Strengths

| Compd | Transition | $R_{\text{exptl}}{}^a$ | $\langle R \rangle^b$ |
|---|---|---|---|
| p-Hydroxy-L-phenylglycine | $^1L_b$ | 0.01 | 0.002 |
| | $^1L_a$ | 0.1 | 0.04 |
| p-Hydroxy-L-phenylglycinamide | $^1L_b$ | 0.01 | 0.003 |
| | $^1L_a$ | 0.05 | 0.04 |

$^a$ As determined from curve fitting to Gaussian band shapes.
$^b$ Average values as determined by a Boltzmann distribution over
the conformational energy surface.

Obviously, the experimental results must depend upon
average values of the rotatory strengths taken over the con-
formational energy surfaces. Thus, the proper method for
comparison of experimental and theoretical results would
be to utilize a Boltzmann distribution to obtain average
values for the rotatory strengths of the electronic transitions
involved. The results of such a procedure are shown in
Table II. The average values which are reported there are in
quite good agreement with experiment. However, this pro-
cedure may not be justified in view of the uncertainties in-
volved in the conformational energy calculations, In fact,
the rather good agreement between the predicted and ob-,
served values of the rotatory strengths may be interpreted
as one step toward the legitimatization of the application of
simple conformational energy calculations such as those
utilized in this work to problems similar to the one under
consideration here.

As was mentioned earlier, the theoretical rotatory
strengths that are associated with the far-ultraviolet transi-
tions of the free amino acid are likely to be unreliable be-
cause the n–$\pi^*$ transition of the carboxylate group has been
omitted from the calculations. However, since the n–$\pi^*$
transition of the amide group was included in the theoreti-
cal optical calculations, the calculated optical properties for
the far-ultraviolet transitions of the amide should be more
reliable.

The theoretical calculations for p-hydroxy-L-phenylgly-
cinamide predict that when the molecule is in the $\psi = -5°$,
$\chi = 70°$ conformation, the two aromatic $^1B$ bands should
give rise to positive and negative Cotton effects at approxi-
mately 195 and 192 nm, respectively. The n–$\pi^*$ transition
of the amide is predicted to yield a positive Cotton effect at
212 nm, whereas the amide $\pi$–$\pi^*$ transition is predicted to
give rise to an intense negative Cotton effect at 183 nm.

It is difficult to quantitatively compare these predictions
for the rotatory strengths of the far-ultraviolet transitions
with experiment because it is not possible to obtain reliable
experimental estimates of the rotatory strengths associated
with each band. Curve fitting methods are unreliable be-
cause there are at least four transitions present in this wave-
length region, and they overlap one another extensively.
Nevertheless, the predicted pattern of rotatory strengths is
definitely consistent with the observed CD spectrum. In ad-
dition, it is of interest that the theoretical methods which
were utilized for these calculations are capable of correctly
predicting that the three lowest energy transitions of these
molecules should give rise to Cotton effects of the same
sign. Since the theory that was used must conserve rotatory
strength over the set of electronic transitions which were in-
cluded in the calculation, it is significant that the predicted
pattern of Cotton effects is consistent with the observed pat-
tern.

There are several significant conclusions that one can
draw from the results of this work. For example, it appears
that the relatively simple theoretical methods which were
employed can semiquantitatively account for the observed

optical activity of molecules of limited conformational free-
dom that include aromatic, carboxylate, and amide chromo-
phores. Furthermore, a significant portion of the rotatory
strength arises from the Kirkwood coupled oscillator mech-
anism, especially in the case of the $^1L_b$ transition. This is
not to imply that other mechanisms are not of potential sig-
nificance; e.g., mechanisms involving the generation of a
local magnetic moment on the aromatic ring by the mixing
of other local transitions could make significant contribu-
tions.[28] However, it is obvious that the simple coupled oscil-
lator mechanism is capable of making significant, and per-
haps dominant, contributions to the optical rotatory power
of aromatic chromophores in amino acids and peptides.
Thus, it is possible that the techniques employed in this
study may be useful for probing the local conformation and
environment of aromatic amino acid residues in protein
molecules.

In addition, the results of this study indicate that p-hy-
droxy-L-phenylglycine and p-hydroxy-L-phenylglycina-
mide are quite hindered insofar as conformational freedom
is concerned and apparently exist in only a restricted num-
ber of conformations which to a first approximation can be
described by the dihedral angles $\psi$ and $\chi$ assuming values
near $-5$ and 75°, respectively. This conformation is very
nearly that which is illustrated in Figure 1. Presumably
phenylglycine itself, and other derivatives thereof, should
assume similar conformations.

**References and Notes**

(1) T. M. Hooker and J. A. Schellman, *Biopolymers*, **9**, 1319 (1970).
(2) T. M. Hooker. P. M. Bayley, W. Radding, and J. A. Schellman, *Biopoly-mers*, **13**, 549 (1974).
(3) J. T. Edsall, P. J. Flory, J. C. Kendrew, A. M. Liquori, G. Némethy, G. N. Ramachandran, and H. A. Scheraga, *Biopolymers*, **4**, 121 (1966); *J. Mol. Biol.*, **15**, 399 (1966).
(4) R. Srinivasan, *Proc. Indian Acad. Sci., Sect. A*, **50**, 19 (1959).
(5) L. Pauling in "Nature of the Chemical Bond," 3rd ed, Cornell University Press, Ithaca, N.Y., 1960.
(6) D. A. Brant, W. G. Miller, and P. J. Flory, *J. Mol. Biol.*, **23**, 47 (1967).
(7) H. A. Scheraga, *Advan. Phys. Org. Chem.*, **6**, 103 (1968).
(8) G. N. Ramachandran and V. Sasisekharan, *Advan. Protein Chem.*, **23**, 283 (1968).
(9) T. Ooi, R. A. Scott, O. Vanderooi, and H. A. Scheraga, *J. Chem. Phys.*, **46**, 4410 (1967).
(10) G. Del Re, *Biochim. Biophys. Acta*, **75**, 153 (1963); *J. Chim. Soc.*, 4031 (1958); *Theor. Chim. Acta*, **1**, 188 (1963).
(11) H. Berthod and A. Pullman, *J. Chim. Phys. Physicochim. Biol.*, **62**, 942 (1965).
(12) D. Poland and H. A. Scheraga, *Biochemistry*, **6**, 3791 (1967).
(13) J. G. Kirkwood, *J. Chem. Phys.*, **5**, 479 (1937).
(14) W. Kuhn, "Stereochemie," K. Freudenberg, Ed., Deuticke, Leipzig, 1933, pp 317–434.
(15) W. Moffitt, *J. Chem. Phys.*, **25**, 467 (1956).
(16) P. M. Bayley, E. B. Nielsen, and J. A. Schellman, *J. Phys. Chem.*, **73**, 228 (1969).
(17) R. W. Woody and I. Tinoco, *J. Chem. Phys.*, **46**, 4927 (1967).
(18) D. Caldwell and H. Eyring, *Rev. Mod. Phys.*, **35**, 577 (1963).
(19) E. G. Hohn and O. E. Weigang, *J. Chem. Phys.*, **48**, 1127 (1968).
(20) E. V. Condon, W. Altar, and H. Eyring, *J. Chem. Phys.*, **5**, 753 (1937).
(21) J. R. Platt, *J. Chem. Phys.*, **17**, 484 (1949).
(22) M. Goeppert-Mayer and A. L. Sklar, *J. Chem. Phys.*, **6**, 645 (1938).
(23) E. E. Barnes and W. T. Simpson, *J. Chem. Phys.*, **39**, 670 (1963).
(24) P. A. Snyder, P. M. Vipond, and W. C. Johnson, *Biopolymers*, **12**, 975 (1973).
(25) E. B. Nielsen and J. A. Schellman, *J. Phys. Chem.*, **71**, 2297 (1967).
(26) D. L. Peterson and W. T. Simpson, *J. Amer. Chem. Soc.*, **79**, 2375 (1957).
(27) J. A. Schellman and E. B. Nielsen, *J. Phys. Chem.*, **71**, 3914 (1967).
(28) A. Moscowitz, A. Rosenberg, and A. E. Hansen, *J. Amer. Chem. Soc.*, **87**, 1813 (1965).